DNA Oxidative Damage by Terpene Catechols as Analogues of Natural Terpene Quinone Methide Precursors in the Presence of Cu(II) and/or NADH

Miguel A. Zuniga, Jifeng Dai, Mark P. Wehunt, and Qibing Zhou*

Department of Chemistry, Virginia Commonwealth University, 1001 West Main Street, Richmond, Virginia 23284-2006

Received January 31, 2006

Natural terpene quinone methides (QM) and their derivatives have been investigated as therapeutics due to their broad antifungal, antibacterial, and antitumor activities. Recently, we reported that a terpene QM was formed from the catechol precursor through the disproportionation of Cu(II)/(I) redox cycle, and extensive DNA damage was observed throughout the oxidation process. In this paper, we investigate DNA damage with a series of terpene catechols as analogues of natural QM precursors and suggest that reactive oxygen species (ROS) are responsible for the observed DNA damage in the Cu^{2+}-induced oxidation despite the stereo- and structural difference of these catechol or subsequent oxidation products. In addition, the presence of NADH significantly enhanced the extent of DNA damage by oxidation of these catechols. Especially with alkene catechols **6**−**7**, the extent of DNA damage was independent of the concentration of catechols, implying that NADH enables the continuous production of ROS through the redox cycle of catechols/quinones.

Introduction

Natural terpene quinone methides (QM)[1] are a category of closely related compounds, and their biological activity attracts numerous research efforts to develop them as effective therapeutics against fungi, bacteria, and tumor growth (*1*−*9*). While many focus on derivatives and analogues of terpene QM (*7*−*9*), we are interested in the biological potential of catechol precursors and their conversion to terpene QMs through an oxidation process. Oxidation of catechol has been well-studied and has significant impacts on biological systems (*10*−*16*). Recently, we reported that terpene QM **1** as an analogue of tingenone (a triterpene QM) was formed from a catechol precursor **2** through the disproportionation of Cu(II)/(I) redox cycle (Scheme 1), and the high reactivity of QM **1** toward nucleophiles was confirmed (*17*). As a result, extensive DNA damage was observed during the oxidation process. Two possible mechanisms may contribute to this observed DNA damage: (1) DNA nucleobase alkylation by in situ generated QM (*18*−*20*) and (2) DNA oxidative damage by reactive oxygen species (ROS) such as superoxide or hydroxyl radical (*13*−*16*). The extent of nucleobase alkylation depends on the stability and reactivity of QM, while ROS are generated from the disproportionation of Cu(II)/(I) redox cycle in the oxidation of catechols (Scheme 1). For catechol oxidation, it has also been reported that NADH (NADPH) can considerably enhance the production of ROS by reducing quinones to catechols, thus, forming a redox cycle with Cu^{2+}-induced oxidation (*13*−*16*, *21*). In this paper, we investigated DNA damage with a series of terpene catechols as analogues of natural QM precursors and suggested that production of ROS was the dominant mechanism for the observed DNA damage in the Cu (II)-induced oxidation

Scheme 1. Diterpenone Catechol 2 as a Precursor for Terpene Quinone Methides Resulted in Extensive DNA Damage in the Presence of Cu^{2+}

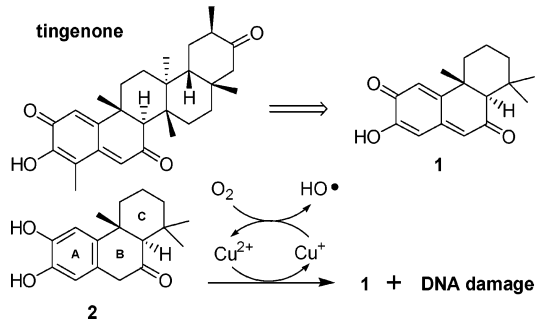

despite the stereo- and structural differences of catechols or subsequent oxidation products. In addition, the extent of DNA damage with alkene analogues increased substantially in the presence of NADH and independent of the concentration, implying that NADH enhances the production of ROS through the redox cycle of catechols/quinones.

To elucidate the Cu^{2+}-induced DNA damage mechanism, a series of catechol analogues of natural terpene QM precursors were designed to investigate potential effects of stereochemistry, substitutional and functional groups on nucleobase alkylation, and production of ROS (Scheme 2). For example, analogue **3** is a diastereoisomer of **2** in a cis-conformation, while all of the reported natural terpene QMs are in the trans-conformation. Interestingly, molecular modeling (Spartan, Wavefunction, Inc., Irvine, CA**)** indicates that analogue **3** adopts a unique bent conformation as compared to that of *trans*-analogue **2** (Figure 1), predicting that the QM of analogue **3** will have a different reactivity toward DNA than **1**. The stability of QM **1** can be improved by incorporating a methyl group on the phenyl ring to prevent potential polymerization (*22*, *23*), which was investigated with analogues **4**−**5**. Also, the QM formation from

* To whom correspondence should be addressed. Phone: (804) 828-3520. Fax: (804) 828-8599. E-mail: qzhou@vcu.edu.

[1] Abbreviations: QM, quinone methide; ROS, reactive oxygen species; DCC, *N*,*N*-dicyclohexylcarbodiimide; NOESY, nuclear Overhauser and exchange spectroscopy; ESI-MS, electrospray ionization mass spectroscopy.

10.1021/tx060021s CCC: $33.50
Published on Web 06/03/2006

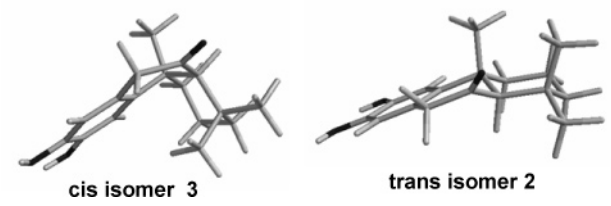

Figure 1. The *cis*-isomer of diterpenone catechol **3** adopts a unique bend structure as compared to that of *trans*-isomer **2**, predicting a different reactivity of QM of **3** in the DNA damage study. Both structures were obtained using AM1 calculation as the molecular modeling method.

Scheme 2. Terpene Catechols 2−7 as Analogues of Natural Terpene QM Precursors

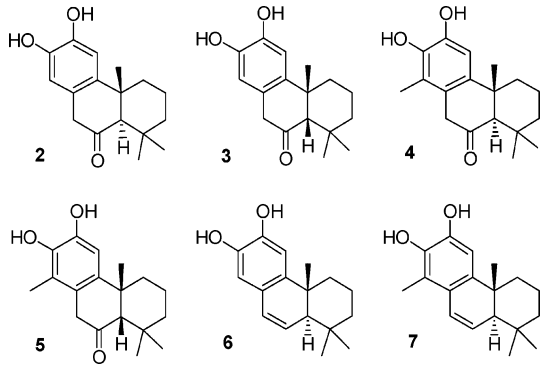

catechol **2** may be unique due to the ketone moiety in the structure (*24*−*26*) and is in contrast to the quinone formation in the oxidation of a variety of catechols (*13*−*16*). Thus, as a comparison, the homoconjugated ketone moiety of catechol **2** was replaced with a conjugated alkene as analogues **6**−**7** for the exclusive formation of quinones (Scheme 2).

Experimental Procedures

All chemicals were purchased from Fisher Scientific (Pittsburgh, PA) or Sigma-Aldrich (Milwaukee, WI) and used without further purification. NMR spectra of the synthesized compounds were obtained by Variant NMR spectrometers. Oligonucleotides were purchased from Invitrogen (Carlsbad, CA) and purified by gel electrophoresis according to published protocols. Aqueous solutions of [γ-32]-ATP (250 μCi) were purchased from MP Biomedicals (Costa Mesa, CA). Gel images of isotopic ^{32}P were obtained by a Molecular Dynamics Typhoon 8600 Variable Mode Imager (Sunnyvale, CA), and water was purified with a Barnstead E-pure 4-Module Deionization System (Dubuque, IA). Electrospray ionization mass spectroscopy (ESI-MS) analysis was carried out using Q-TOF2 from Micromass (Manchester, U.K.). Compounds **2** and **14** and thiol-protected citral were obtained as reported previously (*17*, *27*).

1-(Chloromethyl)-3,4-dimethoxy-2-methylbenzene (9). To a solution of 2-chloroethyl methyl ether (6.05 g, 64.0 mmol) in acetic acid (5.5 mL) was added 2,3-dimethoxytoluene (5.20 mL, 34.7 mmol), and the reaction was initiated by slightly heating. The reaction solution was stirred under N_2 at room temperature for 16 h and then cooled in ice to precipitate the product. The solid was collected by filtration and washed with water. Flash chromatographic separation (5−10% EtOAc in hexanes) afforded the free acid as a white solid (3.21 g) in 47% yield. ^{1}H NMR ($CDCl_3$, 300 MHz): δ 7.04 (d, J = 8.3 Hz, 1H), 6.73 (d, J = 8.3 Hz, 1H), 4.58 (s, 2H), 3.85 (s, 3H), 3.79 (s, 3H), 2.35 (s, 3H). ^{13}C NMR ($CDCl_3$, 75 MHz): δ 153.4, 147.7, 131.9, 129.0, 125.9, 109.5, 60.5, 55.8, 45.6, 11.6. ESI-MS calcd for $C_{10}H_{13}ClO_2$ (M − Cl), 165.09; found, 165.05.

3,4-Dimethoxy-2-methylphenylacetic Acid (10). To a solution of **9** (3.21 g, 16.0 mmol) in dry DMF (35 mL) was added KCN (1.03 g, 1.05 equiv) and 18-crown-6 (5.04 g, 1.2 equiv). The reaction was stirred under N_2 for 16 h. The reaction solution was then extracted with ether (250 mL × 2). The organic layers were collected, dried with $MgSO_4$, and concentrated. Flash chromatographic separation (5−10% EtOAc in hexanes) afforded the cyanide product as an oil (2.81 g) in 92% yield. ^{1}H NMR ($CDCl_3$, 300 MHz): δ 7.02 (d, J = 8.4 Hz, 1H), 6.74 (d, J = 8.4 Hz, 1H), 3.83 (s, 3H), 3.76 (s, 3H), 3.58 (s, 2H), 2.23 (s, 3H). ^{13}C NMR ($CDCl_3$, 75 MHz): δ 152.8, 147.8, 130.6, 124.3, 121.6, 118.1, 109.9, 60.6, 55.9, 21.8, 12.1. ESI-MS calcd for $C_{11}H_{15}NO_2$ (M + H^+), 192.10; found, 192.07.

The cyanide adduct (2.81 g, 14.7 mmol) was refluxed in a solution of NaOH (8.5 g) in ethanol (30 mL) for 18 h. The reaction solution was then acidified with HCl to pH 2 and extracted with CH_2Cl_2 (250 mL × 2). The organic layers were collected, dried with $MgSO_4$, and concentrated. Flash chromatographic separation (2−7% MeOH in CH_2Cl_2) afforded compound **10** as an oil (1.95 g) in 63% yield. ^{1}H NMR ($CDCl_3$, 300 MHz): δ 6.91 (d, J = 8.3 Hz, 1H), 6.72 (d, J = 8.3 Hz, 1H), 3.83 (s, 3H), 3.77 (s, 3H), 3.60 (s, 2H), 2.21 (s, 3H). ^{13}C NMR ($CDCl_3$, 75 MHz): δ 178.4, 152.3, 147.5, 131.6, 126.0, 125.5, 109.7, 60.4, 55.8, 38.9, 12.4. ESI-MS calcd for $C_{11}H_{15}O_4$ (M + H^+), 211.10; found, 211.10.

Methyl (4*E*)-2-(3,4-Dimethoxy-2-methylphenyl)-5,9-dimethyldeca-4,8-dienoate (11). To a solution of freshly distilled diisopropylamine (2.20 mL, 15.7 mmol) in dry THF (20 mL) at −78 °C under N_2 was added a solution of *n*-butyllithium (2.5 M, 6.28 mL). After 10 min at −78 °C, a solution of 3,4-dimethoxyphenylacetic acid (1.40 g, 7.13 mmol) in THF (10 mL) was slowly added. The resulting solution was stirred for 1 h at −78 °C, and then geranyl chloride (1.45 mL, 7.85 mmol) was added. The reaction solution was stirred under N_2 for 18 h and allowed to slowly warm to room temperature. The reaction solution was then quenched with 1 N HCl (250 mL) and extracted with CH_2Cl_2 (250 mL × 2). The organic layers were collected, washed with brine, dried with $MgSO_4$, and concentrated. Flash chromatographic separation (0.5−7% MeOH in CH_2Cl_2) afforded the free acid as a yellow oil (1.65 g) in 70% yield. ^{1}H NMR ($CDCl_3$, 300 MHz): δ 7.06 (d, J = 8.6 Hz, 1H), 6.75 (d, J = 8.6 Hz, 1H), 5.04 (m, 2H), 3.83 (s, 3H), 3.76 (s, 3H), 3.76 (m, 1H), 2.77−2.70 (m, 1H), 2.41−2.34 (m, 1H), 2.29 (s, 3H), 2.00−1.94 (m, 4H), 1.65 (s, 3H), 1.57 (s, 6H). ^{13}C NMR ($CDCl_3$, 75 MHz): δ 180.5, 151.9, 147.2, 137.8, 131.6, 131.2, 130.3, 124.3, 122.8, 120.9, 109.8, 60.5, 55.8, 47.0, 39.9, 31.6, 26.7, 25.8, 17.8, 16.3, 12.1. ESI-MS calcd for $C_{21}H_{31}O_4$ (M + H^+), 347.22; found, 347.22.

To a solution of the resulting free acid (1.57 g, 4.72 mmol) in CH_2Cl_2 (35 mL) were added 4-(dimethylamino)pyridine (681 mg, 1.2 equiv), DCC (1.16 g, 1.2 equiv), and methanol (210 μL, 1.1 equiv). The resulting reaction mixture was stirred under N_2 for 18 h at room temperature. The reaction solution was then quenched with 1 N HCl (250 mL) and extracted with CH_2Cl_2 (250 mL × 2). The organic layers were collected, washed with brine, dried with $MgSO_4$, and concentrated. Flash chromatographic separation (5−20% EtOAc in hexanes) afforded diastereoisomeric pure *trans*-compound **11** as a yellow oil (1.03 g) in 60% yield. ^{1}H NMR ($CDCl_3$, 300 MHz): δ 7.04 (d, J = 8.5 Hz, 1H), 6.74 (d, J = 8.5 Hz, 1H), 5.05−5.00 (m, 2H), 3.83 (s, 3H), 3.77 (s, 3H), 3.76 (m, 1H), 3.64 (s, 3H), 2.76−2.71 (m, 1H), 2.38−2.34 (m, 1H), 2.27 (s, 3H), 2.00−1.93 (m, 4H), 1.66 (s, 3H), 1.57 (s, 6H). ^{13}C NMR ($CDCl_3$, 75 MHz): δ 174.9, 151.7, 147.2, 137.6, 131.6, 130.9, 130.8, 124.3, 122.6, 121.2, 109.7, 60.4, 55.8, 52.0, 47.1, 39.9, 32.1, 26.8, 25.9, 17.8, 16.3, 12.0. ESI-MS calcd for $C_{22}H_{33}O_4$ (M + H^+), 361.24; found, 361.24.

4b,5,6,7,8,8a-*trans*-Hexahydro-2,3-dimethoxy-1,4b,8,8-tetramethylphenanthrenene- (12). To a solution of **11** (992 mg, 2.73 mmol) in dry CH_3NO_2 (20 mL) at −15 °C was added BF_3·Et_2O (2.40 mL, 7 equiv), and the resulting reaction solution was stirred under N_2 at −15 °C for 4 h. The reaction solution was diluted with saturated $NaHCO_3$ (150 mL) and extracted with CH_2Cl_2 (150 mL × 3). The organic layers were collected, washed with brine, dried with $MgSO_4$, and concentrated. Flash chromatographic separation (5−10% EtOAc in hexanes) afforded the diastereoisomeric mixture

of isopropyl ester as a colorless oil (619 mg) in 62% yield. These diastereoisomers were not further separated since one of the chiral centers was removed during the decarboxylation step. ^{1}H NMR ($CDCl_3$, 300 MHz) for the diastereomeric mixture: δ 6.73 (s, 1H), 3.83 (s, 3H), 3.73 (s, 3H), 3.69 (s, 3H), 3.66 (m, 1H), 2.33−2.23 (m, 1H), 2.02 (s, 3H), 1.79−1.17 (m, 11H), 0.94−0.88 (m, 6H). ^{13}C NMR ($CDCl_3$, 75 MHz) observed: δ 177.1, 151.3, 147.1, 145.3, 131.0.3, 123.9, 106.6, 105.9, 60.4, 55.7, 52.3, 48.6, 46.6, 45.2, 44.2, 41.7, 41.3, 39.7, 39.0, 38.0, 33.6, 33.2, 33.0, 25.2, 25.1, 24.7, 24.0, 21.7, 19.5, 19.4, 12.3, 12.1. ESI-MS calcd for $C_{22}H_{33}O_4$ ($M + H^+$), 361.24; found, 361.24.

To a solution of the resulting ester (617 mg, 1.70 mmol) in ethanol (20 mL) was added 3 g crushed NaOH pellets, and the resulting mixture was refluxed for 3 h. The reaction solution was acidified with 2.5 N HCl and extracted with CH_2Cl_2 (150 mL × 3). The organic layers were collected, washed with brine, dried with $MgSO_4$, and concentrated to afford a diastereoisomeric mixture as a viscous oil (432 mg) in 73% yield. ^{1}H NMR ($CDCl_3$, 300 MHz) for the diastereomeric mixture: δ 6.75 (s, 1H), 3.84 (s, 3H), 3.84 (m, 1H), 3.75 (s, 3H), 2.45−2.17 (m, 2H), 2.11 (s, 3H), 1.89−1.18 (m, 10H), 0.96−0.94 (m, 6H). ^{13}C NMR ($CDCl_3$, 75 MHz) observed: δ 182.9, 181.9, 152.1, 151.5, 147.3, 146.9, 145.3, 140.3, 131.1, 125.2, 123.3, 107.2, 106.5, 106.0, 60.5, 60.4, 55.8, 50.3, 48.6, 46.6, 44.8, 44.0, 42.1, 41.8, 41.3, 39.7, 39.0, 38.9, 38.7, 37.9, 37.7, 34.9, 34.4, 33.7, 33.2, 33.0, 32.7, 25.2, 24.6, 24.0, 21.7, 21.7, 19.5, 12.4, 12.0. ESI-MS calcd for $C_{21}H_{31}O_4$ ($M + H^+$), 347.22; found, 347.22.

To the resulting mixture (398 mg, 1.25 mmol), lead(IV) acetate (1.20 g, 2.2 equiv) and copper(II) acetate (248 mg, 1.1 equiv), was added quinoline (15 mL). The resulting dark solution was degassed under vacuum and then heated under N_2 at 140 °C for 3 h. After cooling to room temperature, quinoline from the resulting residue was removed by vacuum distillation. The reaction solution was diluted with 1 N HCl (200 mL) and extracted with CH_2Cl_2 (150 mL × 3). The organic layers were collected, washed with brine, dried with $MgSO_4$, and concentrated. Flash chromatographic separation (5−20% EtOAc in hexanes) afforded product **12** as a colorless oil (200 mg) in 53% yield. ^{1}H NMR ($CDCl_3$, 300 MHz): δ 6.68 (d, J = 2.8 Hz, 1H), 6.64 (s, 1H), 5.95 (d, J = 2.8 Hz, 1H), 3.86 (s, 3H), 3.75 (s, 3H) 2.26 (s, 3H), 2.19−2.07 (m, 2H), 1.75−1.50 (m, 4H), 1.24−1.20 (m, 1H), 1.05 (s, 3H), 1.02 (s, 3H), 0.97 (s, 3H). ^{13}C NMR ($CDCl_3$, 75 MHz): δ 151.9, 145.2, 145.0, 128.4, 127.9, 125.2, 124.2, 104.4, 60.5, 55.9, 50.7, 41.2, 38.5, 36.6, 33.0, 32.7, 22.7, 20.1, 19.3, 11.8. ESI-MS calcd for $C_{20}H_{29}O_2$ (M^+), 300.21; found, 300.09.

4b,5,6,7,8,8a-*trans*-Hexahydro-2,3-dimethoxy-1,4b,8,8-tetramethylphenanthren-9(10*H*)-one (13). To a solution of **12** (270 mg, 0.899 mmol) in CH_2Cl_2 (10 mL) at 0 °C was added *m*-chloroperoxybenzoic acid (70−75%, 443 mg, 1.5 equiv). The resulting reaction solution was stirred at 0 °C under N_2 for 3 h. The reaction solution was quenched with a solution of 5% $Na_2S_2O_3$ and extracted with CH_2Cl_2 (100 mL × 2). The organic layers were collected, washed with brine, dried with $MgSO_4$, and concentrated. The residue was dissolved in $CHCl_3$ (10 mL), and trifluoroacetic acid (0.2 mL) was added. The resulting reaction solution was stirred under N_2 for 18 h and then diluted in CH_2Cl_2 (100 mL). The organic solution was washed with saturated $NaHCO_3$ and brine, dried with $MgSO_4$, and concentrated. Flash chromatographic separation (10−15% EtOAc in hexanes) afforded product **13** as a colorless oil (119 mg) in 41% yield. ^{1}H NMR ($CDCl_3$, 300 MHz): δ 6.76 (s, 1H), 3.85 (s, 3H), 3.76 (s, 3H), 3.46 (d, J = 21.4 Hz, 1H), 3.37 (d, J = 21.4 Hz, 1H), 2.44 (s, 1H), 2.30−2.28 (m, 1H), 2.10 (s, 3H), 1.72−1.64 (m, 4H), 1.43−1.38 (m, 1H), 1.32 (s, 3H), 1.18 (s, 3H), 1.06 (s, 3H). ^{13}C NMR ($CDCl_3$, 75 MHz): δ 209.7, 151.4, 145.8, 144.7, 129.7, 124.0, 105.8, 62.4, 60.5, 56.0, 43.5, 42.8, 41.1, 39.1, 33.0, 32.7, 25.1, 21.8, 19.0, 12.1. ESI-MS calcd for $C_{20}H_{29}O_3$ ($M + H^+$), 317.21; found, 317.20.

4b,5,6,7,8,8a-*trans*-Hexahydro-2,3-dihydroxy-1,4b,8,8-tetramethylphenanthren-9(10*H*)-one (4). To a solution of **13** (11 mg, 0.35 mmol) in CH_2Cl_2 (2.0 mL) under N_2 was added a solution of BBr_3 (1.0 M in heptane, 1.5 mL). The resulting solution was stirred at room temperature for 2 h. The reaction solution was quenched with brine (100 mL) and extracted with degassed EtOAc (100 mL × 2). The organic layers were collected, dried with $MgSO_4$, and concentrated. Flash chromatographic separation (25−35% EtOAc in hexanes) under N_2 afforded product **4** as a brown oil (5.4 mg) in 54% yield. ^{1}H NMR ($CDCl_3$ and CD_3OD, 300 MHz): δ 6.64 (s, 1H), 3.53 (br s, 2H), 3.30 (d, J = 21.3 Hz, 1H), 3.21 (d, J = 21.3 Hz, 1H), 2.39 (s, 1H), 2.17−2.14 (m, 1H), 2.01 (s, 3H), 1.63−1.53 (m, 4H), 1.35−1.30 (m, 1H), 1.24 (s, 3H), 1.02 (s, 3H), 0.97 (s, 3H). ^{13}C NMR ($CDCl_3$ and CD_3OD, 75 MHz): δ 207.5, 138.9, 137.2, 136.8, 118.8, 118.2, 104.0, 58.7, 39.6, 38.8, 36.7, 35.1, 28.9, 28.6, 21.2, 17.7, 15.0, 7.6. ESI-MS calcd for $C_{18}H_{25}O_3$ (M^+), 288.17; found, 288.09.

4b,5,6,7,8,8a-*trans*-Hexahydro-4b,8,8-trimethylphenanthrenene-2,3-diol (6). To a solution of **14** (100 mg, 0.35 mmol) in CH_2Cl_2 (3.0 mL) under N_2 was added a solution of BBr_3 (1.0 M in heptane, 1.5 mL). The resulting solution was stirred at room temperature for 2 h. The reaction solution was quenched with brine (100 mL) and extracted with EtOAc (100 mL × 2). The organic layers were collected, dried with $MgSO_4$, and concentrated. Flash chromatographic separation (25−35% EtOAc in hexanes) under N_2 afforded product **6** as a brown oil (72 mg) in 80% yield. ^{1}H NMR ($CDCl_3$, 300 MHz): δ 6.71 (s, 1H), 6.58 (s, 1H), 6.39 (d, J = 8.7 Hz, 1H), 5.90 (d, J = 8.7 Hz, 1H), 5.14 (br s, 1H), 4.94 (br s, 1H), 2.06 (br m, 2H), 1.72−1.49 (m, 3H), 1.27−1.21 (m, 2H), 1.02 (s, 3H), 0.99 (s, 3H), 0.96 (s, 3H). ^{13}C NMR ($CDCl_3$, 75 MHz): δ 142.9, 142.6, 140.9, 128.8, 126.9, 126.7, 113.8, 110.1, 51.3, 41.2, 37.9, 36.3, 33.0, 32.8, 22.7, 20.5, 19.2. ESI-MS calcd for $C_{17}H_{23}O_2$ (M^+), 258.16; found, 258.08.

4b,5,6,7,8,8a-*trans*-Hexahydro-1,4b,8,8-tetramethylphenanthrenene-2,3-diol (7). To a solution of **13** (32 mg, 0.11 mmol) in CH_2Cl_2 (2.0 mL) under N_2 was added a solution of BBr_3 (1.0 M in heptane, 1.0 mL). The resulting solution was stirred at room temperature for 2 h. The reaction solution was quenched with brine (100 mL) and extracted with EtOAc (100 mL × 2). The organic layers were collected, dried with $MgSO_4$, and concentrated. Flash chromatographic separation (25−35% EtOAc in hexanes) under N_2 afforded product **7** as a brown oil (20 mg) in 68% yield. ^{1}H NMR ($CDCl_3$ and CD_3OD, 300 MHz): δ 6.61 (d, J = 3.0 Hz, 1H), 6.53 (s, 1H), 5.86 (d, J = 2.8 Hz, 1H), 3.51 (br s, 2H), 2.18 (s, 3H), 2.00−1.97 (m, 2H), 1.67−1.42 (m, 3H), 1.21−1.15 (m, 1H), 0.98 (s, 3H), 0.93 (s, 3H), 0.90 (s, 3H). ^{13}C NMR ($CDCl_3$ and CD_3OD, 75 MHz): δ 143.2, 141.6, 140.3, 127.9, 124.5, 124.2, 120.9, 106.9, 50.9, 41.2, 38.0, 36.5, 32.9, 32.7, 22.5, 20.2, 19.2, 11.3. ESI-MS calcd for $C_{18}H_{25}O_2$ (M^+), 272.17; found, 272.09.

General Synthetic Procedures to *cis*-Analogues 3 and 5. To a solution of thiol-protected citral (as a 1:1 cis/trans mixture) in dry THF (20 mL) at −40 °C (acetonitrile/dry ice bath) was slowly added a solution of 1.05 equiv *n*-BuLi (1.6 M in hexanes) under N_2. The resulting reaction solution was stirred at −40 °C for 1 h, and then a solution of 0.95 equiv **15a** or **15b** in dry THF (10 mL) was added. After 4 h, the reaction flask was transferred into a desiccator and kept in a freezer (−25 °C) for 48 h. The reaction solution was quenched with brine (100 mL) and extracted with ether (100 mL × 2). The organic layers were collected, dried with $MgSO_4$, and concentrated. The desired products **16a**,**b** were purified as a cis/trans diastereoisomeric mixture by a flash column separation. Further separation of the isomers was not carried out because the subsequent cyclization step afforded diastereoisomerically pure *cis*-compounds.

To a solution of **16a**,**b** in MeOH/H_2O (9:1, 25 mL) was added 1.1 equiv HgO and $HgCl_2$. The resulting reaction solution was stirred at room temperature for 12 h. The reaction solution was diluted with CH_2Cl_2, and the precipitation was filtered through Celite. The solution was washed with brine, collected, dried with $MgSO_4$, and concentrated. The desired products **17a**,**b** were purified as a cis/trans diastereomeric mixture by a flash column separation.

To a solution of **17a**,**b** in dry CH_3NO_2 (10 mL) at room temperature was added 10 equiv $BF_3{\cdot}Et_2O$, and the resulting reaction solution was stirred under N_2 for 2 h. The reaction solution was diluted with saturated $NaHCO_3$ (150 mL) and extracted with

CH_2Cl_2 (150 mL × 3). The organic layers were collected, dried with $MgSO_4$, and concentrated. The desired compounds **18a**,**b** were purified as a diastereoisomeric pure product by a flash column separation.

To a solution of **18a**,**b** in CH_2Cl_2 (2.0 mL) under N_2 was added a solution of BBr_3 (1.0 M in heptane, 1.0 mL). The resulting solution was stirred at room temperature for 2 h. The reaction solution was quenched with brine (100 mL) and extracted with EtOAc (100 mL × 2). The organic layers were collected, dried with $MgSO_4$, and concentrated. The desired products **3** and **5** were purified by a flash column separation.

2-(3,4-Dimethoxybenzyl)-2-(2,6-dimethylhepta-1,5-dienyl)-1,3-dithiane (16a). A colorless oil: 1.29 g in 63% yield (10−25% EtOAc in hexanes). ^{1}H NMR ($CDCl_3$, 300 MHz) for the cis/trans diastereomeric mixture: δ 6.80−6.77 (m, 3H), 5.40 (s, 1H), 5.15−5.07 (2 sets of triplet, J = 6.7 Hz, 1H), 3.83 (s, 6H), 3.27−3.21 (2 sets of singlet, 2H), 2.92−2.78 (m, 4H), 2.49−2.44 (m, 1H), 2.10−2.05 (m, 5H), 1.80 (2 sets of singlet, 3H), 1.66 (s, 3H), 1.59 (2 sets of singlet, 3H). ^{13}C NMR ($CDCl_3$, 75 MHz) observed: δ 148.2, 142.8, 142.2, 132.0, 131.9, 128.6, 128.4, 128.2, 127.2, 124.4, 124.2, 123.3, 114.4, 110.5, 55.9, 54.8, 54.0, 46.8, 46.5, 41.8, 32.6, 28.1, 27.9, 26.8, 26.3, 25.9, 25.7, 25.6, 24.7, 17.9, 17.2. ESI-MS calcd for $C_{22}H_{33}O_2S_2$ ($M + H^+$), 393.19; found, 393.19.

2-(3,4-Dimethoxy-2-methylbenzyl)-2-(2,6-dimethylhepta-1,5-dienyl)-1,3-dithiane (16b). A colorless oil: 1.18 g in 54% yield (5−25% EtOAc in hexanes). ^{1}H NMR ($CDCl_3$, 300 MHz) for the cis/trans diastereomeric mixture: δ 7.05 (d, J = 8.5 Hz, 1H), 6.67 (d, J = 8.5 Hz, 1H), 5.42 (s, 1H), 5.05 (t, J = 5.4 Hz, 1H), 3.80 (s, 3H), 3.72 (s, 3H), 3.27−3.21 (2 sets of singlet, 2H), 2.97−2.87 (m, 2H), 2.74−2.66 (m, 2H), 2.25 (s, 3H), 2.10−1.96 (m, 6H), 1.66 (s, 3H), 1.62 (s, 3H), 1.58 (s, 3H). ^{13}C NMR ($CDCl_3$, 75 MHz) observed: δ 151.7, 147.2, 142.6, 141.9, 132.4, 131.8, 131.5, 128.5, 127.9, 127.7, 127.6, 127.5, 124.6, 124.4, 108.7, 60.2, 56.0, 55.7, 55.2, 43.7, 43.4, 42.1, 32.0, 28.2, 27.9, 26.6, 26.2, 26.0, 25.9, 25.8, 25.6, 24.9, 17.9, 16.5, 13.4. ESI-MS calcd for $C_{23}H_{35}O_2S_2$ ($M + H^+$), 407.21; found, 407.21.

1-(3,4-Dimethoxyphenyl)-4,8-dimethylnona-3,7-dienyl-2-one (17a). A colorless oil: 125 mg in 62% yield (5−20% EtOAc in hexanes). ^{1}H NMR ($CDCl_3$, 300 MHz) for the cis/trans diastereomeric mixture: δ 6.80−6.71 (m, 3H), 6.07 (s, 1H), 5.10−5.00 (2 sets of multiplet, 1H), 3.84 (s, 6H), 3.62−3.60 (2 sets of multiplet, 2H), 2.57 (t, J = 7.8 Hz, 1H), 2.12−2.09 (5H), 1.83 (s, 1H), 1.64 (s, 3H), 1.56 (s, 3H). ^{13}C NMR ($CDCl_3$, 75 MHz): δ 198.6, 197.9, 160.8, 160.2, 149.1, 148.1, 132.7, 132.3, 127.7, 123.9, 123.1, 122.5, 121.8, 112.7, 111.5, 56.0, 51.3, 41.5, 34.2, 31.8, 26.9, 26.2, 26.0, 25.9, 22.8, 19.7, 17.9, 14.3. ESI-MS calcd for $C_{19}H_{27}O_3$ ($M + H^+$), 303.20; found, 303.08.

1-(3,4-Dimethoxy-2-methylphenyl)-4,8-dimethylnona-3,7-dienyl-2-one (17b). A colorless oil: 156 mg in 50% yield (25−35% EtOAc in hexanes). ^{1}H NMR ($CDCl_3$, 300 MHz) for the cis/trans diastereomeric mixture: δ 6.84 (d, J = 8.3 Hz, 1H), 6.72 (d, J = 8.3 Hz, 1H), δ 6.80−6.71 (m, 3H), 6.07 (s, 1H), 5.10−5.00 (2 sets of multiplet, 1H), 3.82 (s, 3H), 3.76 (s, 3H), 3.64 (s, 2H), 2.60 (t, J = 7.4 Hz, 1H), 2.14−2.11 (m, 8H), 1.84 (s, 1H), 1.66 (s, 3H), 1.57 (s, 3H). ^{13}C NMR ($CDCl_3$, 75 MHz) observed: δ 198.6, 197.8, 160.4, 159.7, 151.8, 147.6, 132.6, 132.2, 131.4, 127.4, 126.0, 123.9, 123.1, 123.0, 122.5, 109.6, 60.4, 55.8, 49.3, 41.4, 34.1, 26.9, 26.2, 26.0, 25.9, 25.8, 19.7, 17.9, 17.8, 12.5. ESI-MS calcd for $C_{20}H_{29}O_3$ ($M + H^+$), 317.21; found, 317.21.

4b,5,6,7,8,8a-*cis*-Hexahydro-2,3-dimethoxy-4b,8,8-trimethylphenanthren-9(10*H*)-one (18a). A colorless oil: 120 mg in 44% yield (25−35% EtOAc in hexanes). ^{1}H NMR ($CDCl_3$, 300 MHz): δ 6.84 (s, 1H), 6.58 (s, 1H), 3.90 (s, 3H), 3.86 (s, 3H), 3.64 (d, J = 23.0 Hz, 1H), 3.54 (d, J = 23.0 Hz, 1H), 2.47−2.42 (m, 1H), 2.09 (s, 1H), 1.58−1.53 (m, 2H), 1.34−1.31 (m, 3H), 1.05 (s, 3H), 0.94 (s, 3H), 0.36 (s, 3H). ^{13}C NMR ($CDCl_3$, 75 MHz): δ 212.7, 148.1, 147.7, 133.7, 126.3, 111.6, 107.8, 66.7, 56.4, 56.1, 43.9, 42.3, 38.6, 36.6, 34.4, 33.6, 32.3, 22.6, 19.1. ESI-MS calcd for $C_{19}H_{27}O_3$ ($M + H^+$), 303.20; found, 303.21.

4b,5,6,7,8,8a-*cis*-Hexahydro-2,3-dimethoxy-1,4b,8,8-tetramethylphenanthren-9(10*H*)-one (18b). A colorless oil: 131 mg in 62% yield (5−10% EtOAc in hexanes). ^{1}H NMR (CD_3CN, 400 MHz): ^{1}H NMR ($CDCl_3$, 300 MHz): δ 6.76 (s, 1H), 3.87 (s, 3H), 3.77 (s, 3H), 3.38 (s, 2H), 2.47−2.43 (m, 1H), 2.10 (s, 3H), 2.08 (s, 1H), 1.58−1.52 (m, 2H), 1.34−1.28 (m, 3H), 1.03 (s, 3H), 0.93 (s, 3H), 0.36 (s, 3H). ^{13}C NMR ($CDCl_3$, 75 MHz): δ 212.6, 151.5, 145.8, 137.1, 130.0, 125.5, 106.0, 66.8, 60.7, 56.1, 42.2, 42.0, 39.1, 36.7, 34.2, 33.9, 32.2, 22.6, 19.1, 12.2. ESI-MS calcd for $C_{20}H_{29}O_3$ ($M + H^+$), 317.21; found, 317.21.

4b,5,6,7,8,8a-*cis*-Hexahydro-2,3-dihydroxy-4b,8,8-trimethylphenanthren-9(10*H*)-one (3). A colorless oil: 16 mg in 72% yield (5−20% EtOAc in hexanes). ^{1}H NMR ($CDCl_3$ and CD_3OD, 300M Hz): δ 6.86 (s, 1H), 6.58 (s, 1H), 5.35 (br, s), 5.33 (br, s), 3.59 (d, J = 23.0 Hz, 1H), 3.39 (d, J = 23.0 Hz, 1H), 2.39−2.35 (d, J = 13.9 Hz, 1H), 2.06 (s, 1H), 1.63−1.48 (m, 2H), 1.33−1.22 (m, 3H), 1.02 (s, 3H), 0.92 (s, 3H), 0.36 (s, 3H). ^{13}C NMR ($CDCl_3$ and CD_3OD, 75 MHz): δ 214.1, 143.3, 142.4, 133.8, 125.7, 115.2, 111.3, 66.7, 43.6, 42.3, 38.4, 36.5, 34.4, 33.6, 32.3, 22.6, 18.9. ESI-MS calcd for $C_{17}H_{23}O_3$ ($M + H^+$), 275.16; found, 275.07.

4b,5,6,7,8,8a-*cis*-Hexahydro-2,3-dihydroxy-1,4b,8,8-tetramethylphenanthren-9(10*H*)-one (5). A colorless oil: 18 mg in 82% yield (25−35% EtOAc in hexanes). ^{1}H NMR ($CDCl_3$, 300 MHz): δ 6.74 (s, 1H), 5.28 (s, 1H), 5.19 (s, 1H), 3.38 (s, 2H), 2.38−2.34 (d, J = 15.0 Hz, 1H), 2.09 (s, 3H), 2.08 (s, 1H), 1.60−1.48 (m, 2H), 1.33−1.22 (m, 3H), 0.99 (s, 3H), 0.92 (s, 3H), 0.37 (s, 3H). ^{13}C NMR ($CDCl_3$, 75 MHz): δ 213.1, 142.1, 140.5, 133.7, 125.4, 122.7, 108.6, 66.7, 42.2, 42.0, 38.6, 36.6, 34.1, 32.2, 22.6, 22.5, 19.0, 11.8. ESI-MS calcd for $C_{18}H_{25}O_3$ ($M + H^+$), 289.18; found, 289.09.

Formation of Diterpenone Quinone and QM under Organic Conditions. The oxidation of catechols was achieved using Ag_2O as an oxidant. After vigorous stirring at ambient temperature for 20 min, the solids were removed by filtration with a 0.2 μm filter (Acrodisc, 13 CR, PTFE). The resulting yellow solution was confirmed as analytically pure QM or quinone by ^{1}H and ^{13}C NMR analysis.

Diterpenone QM **19** (5 mg in 0.8 mL $CDCl_3$). ^{1}H NMR ($CDCl_3$, 300 MHz): δ 6.90 (s, 1H), 6.52 (s, 1H), 6.50 (s, 1H), 6.31 (s, 1H), 2.25 (m, 1H), 2.23 (s, 1H), 1.61−1.44 (m, 2H), 1.35−1.23 (m, 3H), 1.18 (s, 3H), 0.95 (s, 3H), 0.61 (s, 3H). ^{13}C NMR ($CDCl_3$, 75 MHz): δ 201.8, 182.1, 155.6, 149.9, 143.2, 132.3, 122.1, 111.0, 66.9, 41.9, 41.5, 36.3, 35.8, 35.5, 31.0, 24.7, 18.5.

Diterpenone quinone **20** (5 mg in 0.8 mL $CDCl_3$). ^{1}H NMR (300 MHz): δ 6.54 (d, J = 2.2 Hz, 1H), 6.52 (d, J = 2.2 Hz, 1H), 6.20 (s, 1H), 6.12 (s, 1H), 2.11 (s, 1H), 2.03 (d, J = 12.1 Hz, 1H), 1.75−1.72 (m, 2H), 1.58−1.54 (m, 1H), 1.26−1.14 (m, 2H), 1.21 (s, 3H), 1.03 (s, 3H), 1.01 (s, 3H). ^{13}C NMR ($CDCl_3$, 75 MHz): δ 181.4, 180.7, 163.8, 145.0, 143.4, 127.3, 123.2, 121.6, 51.0, 41.5, 40.4, 35.7, 33.5, 32.9, 22.5, 22.5, 18.6.

DNA Oxidative Damage of Diterpenone Catechols 2−7 in the Presence of $CuCl_2$. The 30-mer oligonucleotide of the DNA target was radiolabeled with ^{32}P-phosphate at the 5′-position by T4 polynucleotide kinase (New England Biolabs, MA) according to the manufacturer's instructions. Hybridization of complementary strands was achieved by heating a solution of oligonucleotides (0.5 μM each, 0.28 μCi/μL) in a 90 °C water bath and then cooling to room temperature slowly. A series of reaction solutions containing compounds **2**−**7** were prepared, and the DNA lesion was initiated by the addition of the catechols. The final reaction solutions (10 μL each) contained 0.25 μM duplex DNA (0.07 μCi/μL), 10 mM phosphate buffer (pH 7.0), 1 mM $MgCl_2$, $CuCl_2$ (40 μM), compounds **2**−**7** (0, 10, 20, 30, and 40 μM, respectively), and 10% acetonitrile. The resulting reaction solutions were incubated at 37 °C for 12 h. A portion of the reaction solutions (0.1 μCi) was mixed with formamide and directly separated by a 20% denatured PAGE for the investigation of direct DNA cleavage. The piperidine treatment was achieved by mixing the reaction solutions with a 10% piperidine in water (100 μL) and then heating at 90 °C for 20 min. The resulting solutions were lyophilized, and the residues were dissolved in 90% formamide loading buffer. Each reaction solution (0.15 μCi) was separated by 20% denatured PAGE and analyzed by gel image analysis software. The percentage of DNA damage

Scheme 3. Synthesis of *trans*-Terpene Catechol Analogues

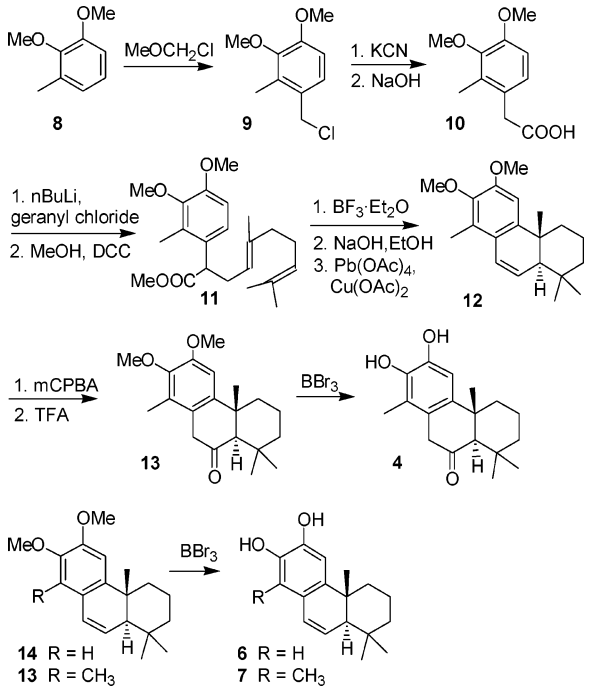

Scheme 4. Synthesis of *cis*-Terpene Catechol Analogues

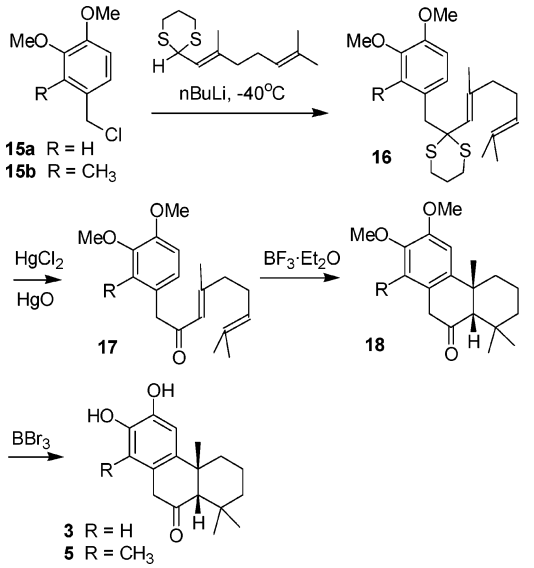

was calculated based on the amount of the originally radiolabeled DNA band versus the total amount of radioactive DNA using the quantitative analysis software provided by the imager manufacturer. The DNA oxidative damage by free radicals using Fe^{3+}-EDTA and H_2O_2 was carried out according to the published protocol (*28*). The investigation of the effect by radical scavengers and copper chelators on the DNA damage with terpenone **2** and Cu^{2+} was carried out similarly as described above. The final concentrations for compound **2** and $CuCl_2$ were 20 μM each. The concentrations of radical scavengers and chelators used were 5% for ethanol, 0.1 M for mannitol, 0.1 M for sodium formate, 5% for DMSO, 1.5 unit/10 μL for superoxide dismutase, 1.5 unit/10 μL for catalase, 50 μM for bathacuproine, and 0.1 M for methional, respectively. The piperidine treatment was carried out after incubating the reaction mixtures at 37 °C for 10 h. All the experiments were repeated at least three times independently.

DNA Oxidative Damage of Diterpenone Catechols 2−7 in the Presence of $CuCl_2$ and NADH. A series of reaction solutions containing compounds **2**−**7** were prepared similarly as described above. The duplex DNA solution was mixed with a solution of $CuCl_2$ and NADH first, and then followed by the addition of catechol solutions. The final reaction solutions (20 μL each) contained 0.25 μM duplex DNA (0.07 μCi/μL), 10 mM phosphate buffer (pH 7.0), 1 mM $MgCl_2$, 100 μM NADH, $CuCl_2$ (5 μM), compounds **2**−**7** (0, 0.5, 1, 2, and 5 μM, respectively), and 5% acetonitrile. The resulting reaction solutions were incubated at 37 °C for 6 h. The piperidine treatment and subsequent PAGE separation were carried out similarly as described above. All the experiments were repeated at least three times independently.

Result and Discussion

Synthesis of Terpene Catechols. The *cis*- and *trans*-catechols **2**−**7** were synthesized diastereoselectively using a Lewis-acid-catalyzed polyene cyclization. The *trans*-isomers **2**, **4**, and **6**−**7** were formed selectively through cyclization of ester derivatives of polyenes such as derivative **11** (Scheme 3), as reported previously (*7*, *17*). Interestingly, we found that if one of the double bonds of polyenes was conjugated with a carbonyl group as in compound **17** (Scheme 4), cyclization afforded the *cis*-isomer dominantly. This unique diastereoisomeric selectivity not only enabled us to obtain *cis*-conformational analogues, but also implied a different mechanism in the cyclization of conjugated polyenes, possibly involving an enolate intermediate. The synthesis is summarized in Schemes 3 and 4.

Synthesis of *trans*-catechols **2**, **4**, and **6**−**7** was accomplished through the ester-derivative cyclization pathway. Catechol **2** was obtained as reported previously (*17*), and the synthesis of **3** was carried out similarly except starting from a methylated carboxylic acid **10** (Scheme 3). For acid **10**, 2,3-dimethoxytoluene was first converted to benzyl chloride **9** (*29*), followed by cyanide addition and then hydrolysis in NaOH solutions (*30*) to the desired acid in an overall yield of 27%. Subsequent synthetic steps to **4** included coupling with geranyl chloride, ester formation, $BF_3{\cdot}OEt_2$ cyclization, hydrolysis, decarboxylation, oxidation, and deprotection, which were carried out similarly as described for catechol **2** (*17*). We found that all of the steps afforded reasonable yields except that a methyl ester **11**, instead of the isopropyl ester, must be used in the polyene cyclization, possibly to reduce the steric bulkiness around the aromatic ring. Catechols **6**−**7** were obtained directly from the deprotection of the alkene intermediates **13**−**14** from the synthesis of analogues **2** and **4** (Scheme 3).

cis-Analogues **3** and **5** were obtained using the conjugated polyene synthetic approach (Scheme 4). First, dimethoxylbenzyl chloride **15** was coupled with *n*-BuLi and 1,3-dithiol-protected citral (1:1 cis/trans isomers) at −40 °C to compound **16** as a diastereoisomeric mixture in 54−63% yield (*29*). The thiol groups were then removed with $HgCl_2$ and HgO in a 9:1 MeOH−water solution in 55−62% yield (*31*). The resulting polyene **17** as a diastereoisomeric mixture was cyclized in the presence of $BF_3{\cdot}OEt_2$, affording the *cis*-isomers diastereoisomeric selectively. The cis-conformation of the resulting diterpenone **18** was confirmed by 2-D NMR NOESY analysis (see Supporting Information). Finally, methyl ethers of **15** were removed with BBr_3 to the desired *cis*-catechol analogues (*17*).

During the synthesis, we noticed that compounds with the same conformation had similar ^1H NMR chemical shifts of methyl groups on the C-ring (Scheme 1). For example, the chemical shifts of three methyl groups of *cis*-isomers **3**, **5**, and **18** are at approximately 1.02, 0.93, and 0.36 ppm, respectively, while those of *trans*-isomers **6**, **7**, and **12**−**14**, are between 1.32 and 0.97 ppm. These unique chemical shifts may be helpful to confirm the stereo-conformation of terpene isomers.

Quinone Methide and *o*-Quinone Formation upon Oxidation. Both *p*-QM and *o*-quinone were obtained upon oxidation

Scheme 5. Formation of QMs or Quinones of Terpene Catechols upon Oxidation

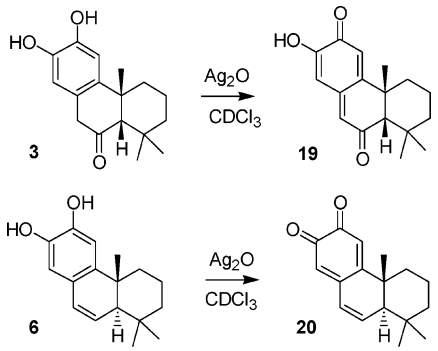

of catechols **3** and **6**, respectively (Scheme 5). This was consistent with our previously reported QM formation and also confirmed the exclusive formation of quinones from catechol **6** in our design.

Oxidation of *cis*-catechol **3** with Ag_2O in $CDCl_3$ afforded analytically pure *p*-QM **19**, which was confirmed by both ^1H and ^{13}C NMR analysis (*17*, *23*). In the ^1H NMR spectrum, the signals of benzylic protons of **3** at 3.5 ppm disappeared completely upon oxidation, while four singlets were observed between 6.31 and 6.90 ppm (see Supporting Information). Also, the ^{13}C spectrum showed 8 carbon signals in the region above 100 ppm and 9 below 70 ppm as compared to 7 and 10 of catechol **3**. All of these spectral analyses are consistent with the exclusive conversion of catechol **3** to *p*-QM **19** (*17*, *23*).

In contrast to the high reactive *p*-QM **1** as we previously reported, *p*-QM **19** of the *cis*-catechol **3** remained unchanged upon concentration and storage over several weeks at −4 °C. On the other hand, flash chromatography with silica gel completely degraded *p*-QM **19**. The exceptional stability of *p*-QM **19** can be attributed to its unique bent cis-conformation versus the relative flat trans-conformation of **2** (Figure 1), which may effectively prevent polymerization upon concentration.

o-Quinone **20** was formed exclusively in the oxidation of catechol **6** and also confirmed by both ^1H NMR and ^{13}C NMR analysis. The conjugated *o*-quinone **16** remained unchanged over 3 days by ^1H NMR analysis, however, polymerized upon concentration. Therefore, these results indicated that *p*-QMs formations are unique to homo-conjugated catechols as the oxidation products, while *o*-quinones are formed preferably for simple catechols or conjugated catechols.

DNA Damage by Catechols 2−7 in the Presence of Cu^{2+}. DNA damage was observed by all of catechol analogues in the presence of Cu^{2+} to various extents, possibly due to the stereo-, substitutional, and functional group effects. More importantly, analysis of DNA damage after piperidine treatment showed an identical fragment pattern, which is similar to that of the oxidative damage by H_2O_2/Fe(III)-EDTA. These results suggested that production of ROS in the Cu(II)-induced oxidation of catechols is the predominant cause for the observed DNA damage.

For analysis of DNA damage, a ^{32}P-radiolabeled oligonucleotide duplex target was selected as described previously (*17*) and treated with catechols **2**−**7** (10−40 μM) and 40 μM Cu^{2+} at 37°C for 12 h (Figure 2). Gel electrophoresis analysis of both nonpiperidine- and piperidine-treated reactions were carried out similarly as described previously (*17*). While the analysis of nonpiperidine-treated reactions showed direct cleavage of the DNA strand (see Supporting Information), the analysis of piperidine-treated ones indicated not only DNA strand cleavage but also nucleobase depurinations due to oxidation and alkylation (*13*−*16*, *32*). As shown in Figure 2, the extent of DNA damage after piperidine treatment was concentration-dependent within each compound yet varied from one another. The percentage of undamaged DNA was calculated based on the

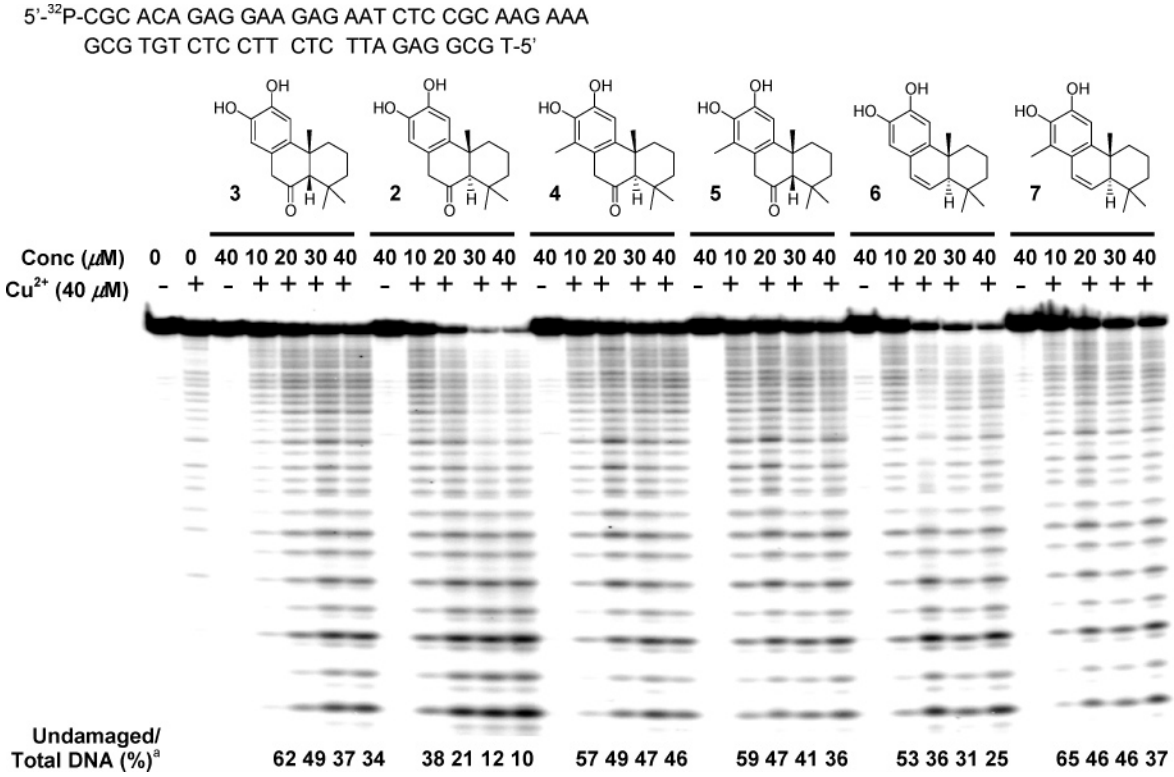

Figure 2. DNA damage with compounds **2**−**7** in the presence of Cu^{2+} after piperidine treatment. The concentration of duplex DNA was 0.25 μM in 10 mM phosphate buffer (pH 7.40) and 1 mM $MgCl_2$. [a]The percentage was calculated as the average from three independent experiments using the amount of undamaged radiolabeled DNA versus the total amount of radioactive DNA. The average standard deviation was 5%.

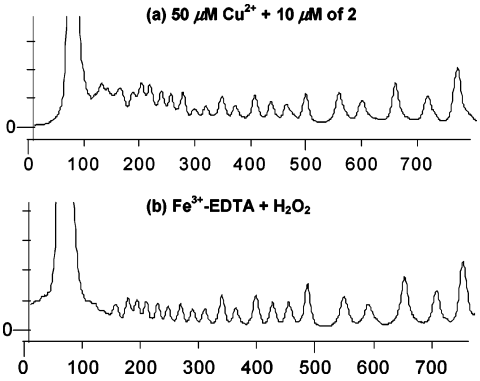

Figure 3. Identical fragment pattern was observed in the DNA damage by Cu^{2+}-induced oxidation of catechols versus that by hydroxyl radical, revealing ROS as the DNA damaging mechanism. DNA fragment patterns were obtained with (a) **2** at 10 μM; (b) Fe^{3+}-EDTA and H_2O_2.

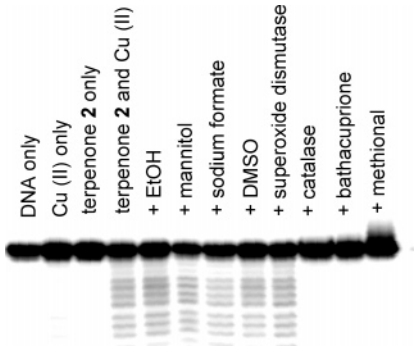

Figure 4. The effect of radical scavengers and copper chelators on DNA damage by diterpenone **2** (20 μM) and Cu^{2+} (20 μM) after piperidine treatment. The concentration of duplex DNA was 0.25 μM in 10 mM phosphate buffer (pH 7.40) and 1 mM $MgCl_2$. The concentrations for radical scavengers and chelators were 5% for ethanol, 0.1 M for mannitol, 0.1 M for sodium formate, 5% for DMSO, 1.5 unit/10 μL for superoxide dismutase, 1.5 unit/10 μL for catalase, 50 μM for bathacuproine, and 0.1 M for methional, respectively.

amount of originally labeled DNA versus the total amount of radioactive fragments in the phosphor-imaging analysis. On the basis of the percentage of undamaged DNA, *trans*-catechols **2** and **6** have higher amount of DNA damage than other analogues at the same concentrations. When comparing catechol **2** to **4**, the additional methyl group on the A-ring decreased the amount of DNA damage significantly, and moderated decrease was observed in the case of catechols **6** to **7** (Figure 2). On the other hand, the methyl effect was not observed on the *cis*-analogues **3**−**4**, while the amount of DNA damage by *cis*-catechol **3** was much lower than that by *trans*-catechol **2**, probably due to its unique bent cis-conformation. These results implied that the extent of DNA damage with catechols **2**−**7** was possibly due to steric effects on interactions between Cu^{2+} and catechol (*15*, *16*), although a more thorough computational study is needed to verify this.

Despite the different extent of DNA damage, all of the catechols **2**−**7** induced a similar fragment pattern as shown in Figure 2. When compared with the same percentage of DNA damage, almost identical patterns were observed (Figure 2), that is, DNA damage with 30 μM of **3**, 10 μM of **2**, and 20 μM of **6**. The similarity of the fragment pattern indicated that DNA damage was due to a common mechanism in the presence of Cu^{2+}. On the basis of the Cu^{2+}-induced oxidation mechanism, the common product from these analogues were ROS generated through the disproportion of Cu(II)/(I) redox cycle (*13*−*16*). Thus, the fragment pattern from Cu^{2+}-induced oxidation of catechols was compared to that of DNA damage by H_2O_2/Fe^{3+}-EDTA and was found to be identical (Figure 3). These results suggested that the observed DNA fragment pattern with catechols **2**−**7** was due to the nonselective DNA damage by radical species (*28*). In addition, the mechanism of catechol oxidation with Cu^{2+} has been well-established over recent years using radical scavenge studies and EPR analysis (*13*−*16*), which indicated many ROS were involved including $O_2^{\bullet-}$, Cu(I)-OOH, $HO^{\bullet}$, and H_2O_2. The DNA damage mechanism was proposed

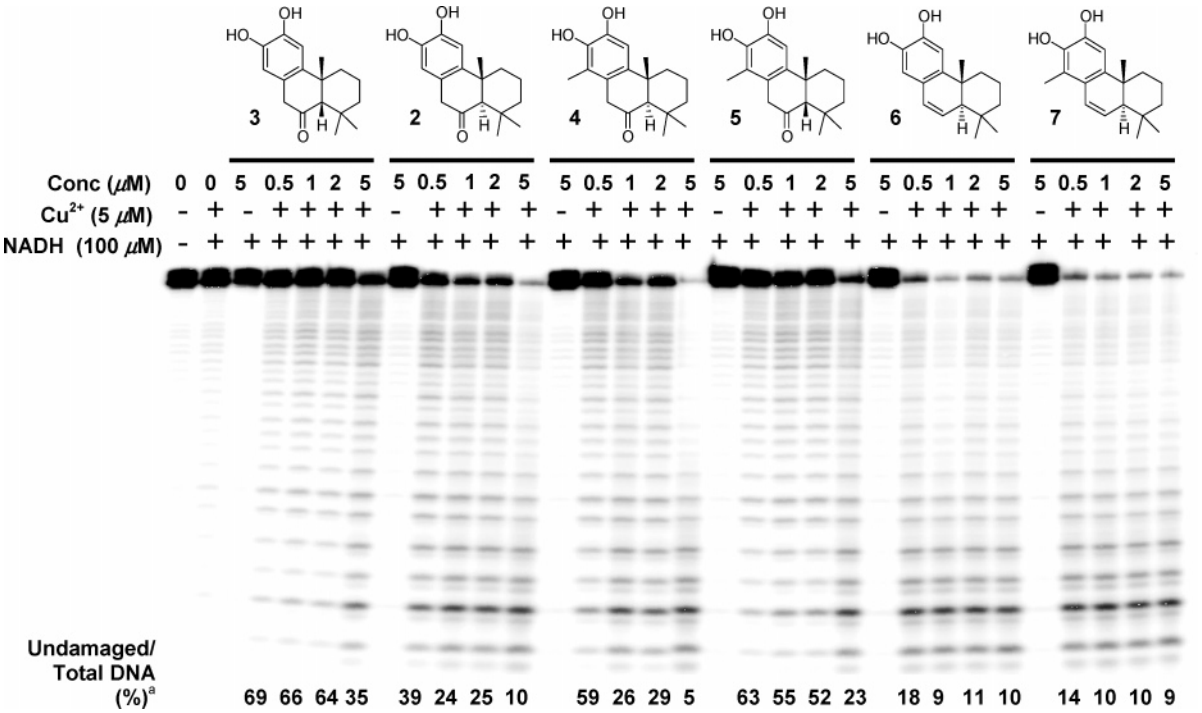

Figure 5. Enhanced DNA damage in the presence of 100 μM NADH and 5 μM Cu^{2+} with compounds **2**−**7** at concentrations of 0.5−5 μM after piperidine treatment. The concentration of duplex DNA was 0.25 μM in a 10 mM phosphate buffer (pH 7.40) and 1 mM $MgCl_2$. [a]The percentage was calculated using the amount of undamaged radiolabeled DNA versus the total amount of radioactive DNA, and the average standard deviation was 5%. All the reactions were repeated three independent times.

to occur via the in situ released HO• from the DNA−Cu(I)−OOH complex. This Cu(I)−radical complex mechanism was further verified by the study of the effect of radical scavengers and copper chelators on the observed DNA damage with diterpenone **2** and Cu^{2+} (Figure 4). Consistent to reported studies (*13*−*16*), free HO• radical scavengers including ethanol, mannitol, formate, and DMSO had no effects on the extent of DNA damage. While in contrast, catalase, bathocuproine, and methional completely quenched the observed oxidative damage on DNA. These results further supported that the oxidation of catechol derivatives through disproportionation of Cu(II)/Cu(I) is different from the free radical mechanism of Fe(III)-H_2O_2, although similar DNA damaging patterns were observed.

Although nucleobase adducts could be formed with reactive QMs or quinones in the oxidation process, this was not observed under the conditions studied on the basis of the similar DNA fragment pattern by catechols **2**−**7** versus that by H_2O_2/Fe^{3+}-EDTA. An alternative reaction pathway for the formed QMs and quinones could be competitive water addition, which was observed in the nucleobase alkylation with QMs (*18*, *20*). Therefore, these results suggested that production of ROS was the dominant mechanism for DNA damage in the Cu^{2+}-induced oxidation, regardless of the structural difference of catechols and subsequent oxidation products as QM or quinone.

DNA Damage by Catechols 2−7 with NADH and Cu^{2+}. In the presence of NADH, DNA damage by the Cu^{2+}-induced oxidation of catechols **2**−**7** occurred to a higher extent at lower concentrations. With alkene catechols **6**−**7**, the extent of DNA damage was enhanced substantially, implying that NADH enabled the generation of ROS through the redox cycle of catechols/quinones.

For the assessment of DNA damage, the radiolabeled DNA target was treated with catechols **2**−**7** at 0.5−5 and 5 μM Cu^{2+} in the presence of 100 μM NADH to mimic the reducing environment by NADPH under biological conditions (*14*−*16*, *21*). After incubation for 6 h at 37 °C, reactions were treated with piperidine, and gel electrophoresis analysis was carried out similarly as described. The gel image showed a similar fragment pattern to that without NADH. However, the extent of DNA damage varied significantly (Figure 5). For both alkene catechols **6**−**7**, more than 80% of the original DNA was damaged. The extent of DNA damage was not concentration-dependent, especially when comparing 1 versus 5 μM. On the other hand, DNA damage with *trans*-catechols **2** and **4** was higher than that with *cis*-catechols **2**−**5** in a concentration-dependent manner, although the methyl effect was not obvious.

The enhanced DNA damage with NADH in the Cu^{2+}-induced oxidation of catechols **2**−**7** was attributed to the reducing capability of NADH (*14*−*16*, *21*). Both NADH and NADPH have been shown to be able to reduce the oxidized quinones back to the original catechols, forming a redox cycle with catechol oxidation (Scheme 6). In our study, the concentration-dependent DNA damage with catechols **2**−**5** implied that NADH might reduce the oxidation products only partially. Thus, production of ROS was higher than that without NADH. On the other hand, the extent of DNA damage by alkene catechols **6** and **7** was not concentration-dependent. This suggested that NADH was able to reduce the formed quinones fully to the initial catechol, forming a complete redox cycle of catechol/quinone with Cu^{2+}-induced oxidation (Scheme 6). As a result, disproportion of Cu(II)/(I) with oxygen continuously produced ROS until all of NADH was fully consumed.

In conclusion, we have demonstrated that ROS are possibly the dominant cause of DNA damage in Cu^{2+}-induced oxidation of catechols regardless of structural differences and oxidation products. The observed substantial DNA damage by alkene catechols **6**−**7** in the presence of NADH revealed their potential detrimental effects in cells upon oxidation. These results provided a fundamental basis for future biological studies on the oxidative metabolism of terpene catechols and may further contribute the understanding of neoplastic development by natural catechol carcinogens.

Scheme 6. The Redox Cycle of *trans*-Terpene Catechol/Quinone through Cu^{2+} and NADH

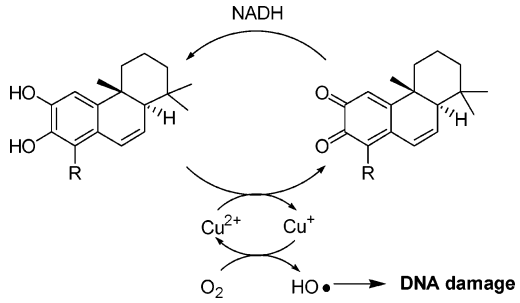

Acknowledgment. We thank the financial support (startup fund) from Virginia Commonwealth University. We also thank John B. Mangrum for his help on the mass analysis.

Supporting Information Available: NMR spectra of compounds **3**−**20** and the gel image of direct DNA cleavage by compounds **2**−**7** (24 pages). This material is available free of charge via the Internet at http://pubs.acs.org.

References

(1) Topcu, G., Altiner, E. S., Gozcu, S., Halfon, B., Aydogmus, Z., Pezzuto, J. M., Zhou, B.-N., and Kingston, D. G. I. (2003) Studies on di- and triterpenoids from *Salvia staminea* with cytotoxic activity. *Planta Med. 69*, 464−467.

(2) Setzer, W., Holland, M., Bozeman, C. A., Rozmus, G. F., Setzer, M. C., Moriarity, D. M., Reeb, S., Vogler, B., Bates, R. B., and Haber, W. A. (2001) Isolation and frontier molecular orbital investigation of bioactive quinone-methide triterpenoids from the bark of *Salcia petenensis*. *Planta Med. 67*, 65−69.

(3) Ulubelen, A., ÖKsöz, S., Kolak, U., Bozok-Johansson, C., Celik, C., and Voelter, W. (2000) Antibacterial diterpenes from the roots of *Salvia viridis*. *Planta Med. 66*, 458−462.

(4) Chávez, H., Estévez-Braum, A., Ravelo, A. G., and González, A. G. (1999) New phenolic and quinone-methide triterpenes from *Maytenus amazonia*. *J. Nat. Prod. 62*, 434−436.

(5) Alvarenga, N. L., Velázquez, C. A., Gómez, R., Canela, N. J., Bazzocchi, I. L., and Ferro, E. A. (1999) A new antibiotic nortriterpene quinone methide from *Maytenus catingarum*. *J. Nat. Prod. 62*, 750−751.

(6) González, A. G., Alvarenga, N. L., Bazzocchi, I. L., Ravelo, A. G., and Moujir, L. (1998) A new bioactive norquinone methide triterpene from *Maytenus scutioides*. *Planta Med. 64*, 769−771.

(7) Yang, Z., Kitano, Y., Chiba, K., Shibata, N., Kurokawa, H., Doi, Y., Arakawa, Y., and Tada, M. (2001) Synthesis of various oxidized abietane diterpenes and their antibacterial activities against MRSA and VRE. *Bioorg. Med. Chem. 9*, 347−356.

(8) Tada, M., Nishiiri, S., Yang, Z., Imai, Y., Tajima, S., Okazaki, N., Kitano, Y., and Chiba, K. (2000) Synthesis of (+)- and (−)-ferruginol via asymmetric cyclization of a polyene. *J. Chem. Soc., Perkin Trans. 1*, 2657−2664.

(9) Revelo, A. G., Estevez-Braun, A., Chavez-Orellana, H., Perez-Sacau, E., and Mesa-Siverio, D. (2004) Recent studies on natural products as anticancer agents. *Curr. Topics Med. Chem. 4*, 241−265.

(10) Jiang, H., Vudathala, D. K., Blair, I. A., and Penning, T. M. (2006) Competing roles of aldo-keto reductase 1A1 and cytochrome P4501B1 in benzo[*a*]pyrene-7,8-diol activation in human bronchoalveolar H358 cells: role of AKRs in P4501B1 induction. *Chem. Res. Toxicol. 19*, 68−78.

(11) Liu, X., Yao, J., Pisha, E., Yang, Y., Hua, Y., van Breeman, R. B., and Bolton, J. L. (2002) Oxidative DNA damage induced by equinine estrogen metabolites: role of estrogen receptor α. *Chem. Res. Toxicol. 15*, 512−519.

(12) Sugumaran, M., Duggaraju, P., Jayachandran, E., and Kirk, K. L. (1999) Formation of a new quinone methide intermediate during the oxidative transformation of 3,4-dihydroxyphenylacetic acids: implication for eumelanin biosynthesis. *Arch. Biochem. Biophy. 371*, 98−106.
(13) Hirakawa, K., Oikawa, S., Hirosawa, I., Hirosu, I., and Kawanishi, S. (2002) Catechol and hydroquinone have different redox properties responsible for their differential DNA-damaging ability. *Chem. Res. Toxicol. 15*, 76−82.
(14) Oikawa, S., Hirosawa, I., Hirakawa, K., and Kawanishi, S. (2001) Site specificity and mechanism of oxidative DNA damage induced by carcinogenic catechol. *Carcinogenesis, 22*, 1239−1245.
(15) Schweigert, N., Acero, J. L., von Gunten, U., Canonica, S., Zehnder, A. J. B., and Eggen, R. I. L. (2000) DNA degradation by the mixture of copper and catechol is caused by DNA-copper-hydroperoxo complexes, probably DNA-Cu(I)OOH. *Environ. Sci. Mol. Mutagen. 36*, 5−12.
(16) Flowers, L., Ohnishi, T., and Penning, T. M. (1997) DNA strand scission by polycylic hydrocarbon *o*-quinone: role of reactive oxygen species, Cu(II)/(I) redox cycling, and *o*-semiquinone anion radicals. *Biochemistry 36*, 8640−8648.
(17) Zhou, Q., and Zuniga, M. A. (2005) Quinone methides formations in the Cu^{2+}-induced oxidation of a diterpenone catechol and concurrent damage on DNA. *Chem. Res. Toxicol*. *18*, 382−388.
(18) Pande, P., Shearer, J.; Yang, J., Greenberg, W. A., and Rokita, S. E. (1999**)** Alkylation of nucleic acids by a model quinone methide. *J. Am. Chem. Soc. 121*, 6773−6779.
(19) Bolton, J. L., Pisha, E., Zhang, F., and Qiu, S. (1998) Role of quinoids in estrogen carcinogenesis. *Chem. Res. Toxicol. 10*, 1113−1127.
(20) Thopmson, D. C., Thopmson, J. A., Sugumaran, M., and Moldeus, P. (1992) Biological and toxical consequences of quinone methide formation. *Chem.−Biol. Interact. 86*, 129−162.
(21) Seike, K., Murata, M., Oikawa, S., Hiraku, Y., Hirakawa, K., and Kawanishi, S. (2003) Oxidative DNA damage induced by benz[*a*]-anthracene metabolites via redox cycles of quinone and unique non-quinone. *Chem. Res. Toxicol. 16*, 1470−1476.
(22) Volod′kin, A. A., and Ershov, V. V. (1988) Stable methylenequinones. *Russ. Chem. Rev. 57*, 336−349.
(23) Lycka, A., Snobl, D., Koutek, B., Pavlickova, L., and Soucek, M. (1981) ^{13}C NMR study of substituted quinone methides: a study of the *ortho*-effect. *Collect. Czech Chem. Commun. 46*, 1775−1787.
(24) Iverson, S. L., Hu, L. Q., Vukomanovic, V., and Bolton, J. L. (1995) The influence of the *p*-alkyl substituent on the isomerization of *o*-quinones to *p*-quinone methides: potential bioactivation mechanism for catechols. *Chem. Res. Toxicol. 8*, 537−544.
(25) Bolton, J. L., Acay, N. M., and Vukomanovic, V. (1994) Evidence that 3-allyl-*o*-quinone spontaneously rearrange to their more electrophilic quinone methides: potential bioactivation mechanism for the hepatocarcinogen safrole. *Chem. Res. Toxicol. 7*, 443−450.
(26) Sugumaran, M., Saul, S., and Semensi, V. (1989) Trapping of transiently formed quinone methide during enzymatic conversion of *N*-acetyldopamine to *N*-acetylnorepinephrine. *FEBS Lett*. *252*, 135−138.
(27) Scheller, M. E., Iwasaki, G., and Frei, B. (1986) Photochemical reactions. 148. Photochemistry of acylsilanes: preparation, photolyses, and thermolyses of α,β-unsaturated silyl ketones. *Helv. Chim. Acta 69*, 1378−1394.
(28) Tallius, T. D. (2000) Probing DNA structure with hydroxyl radicals. In *Current Protocols in Nucleic Acid Chemistry* (Beaucage, S. L., Bergstrom, D. E., Glick, G. D., and Jones, R. A., Eds.) p 6.7.1−6.7.8, Wiley & Son, New York.
(29) Wei, W.-G., and Yao, Z.-J. (2003) A practical procedure for multisubstituted β-naphthols and their derivatives. *Tetrahedron 59*, 6621−6625.
(30) Aristoff, P. A., Johnson, P. D., and Harrison, A. W. (1985) Total synthesis of a novel antiulcer agent via a modification of the intramolecular Wadsworth-Emmons-Wittig reaction *J. Am Chem. Soc. 114, 107*, 7967−7974.
(31) Soderquist, J. A., and Miranda, E. I. (1992) Formyl(triisopropyl)-silane: the synthesis and chemistry of a stable formylsilane. *J. Am Chem. Soc. 114*, 10078−10081.
(32) Zhou, Q., Pande, P., Johnson, A. E., and Rokita, S. E. (2001) Sequence specific delivery of a quinone methide intermediate to the major groove of DNA. *Bioorg. Med. Chem. 9*, 2347−2354.

TX060021S